

Figure S1. Expression, structure and sequence of *C. elegans* HP1 proteins. (A) Representative microscopy images of mKate2::HPL-1 and mKate2::HPL-2 nuclear expression in the hypodermis (left panel) and intestine (right panel). mKate is shown in magenta, nuclear membrane is labelled by GFP::MEL-28. Bar: 5μm. (B) RNAseq expression data of the different *hpl-2* isoforms (framed in red) from WormBase Genome Browser. Neighboring genes are also shown. (C) Schematic representation of Chromodomain (CD), Chromo Shadow Domain (CSD) and Hinge region (H) in HPL-1 unique isoform and HPL-2 a, b and c isoforms. (D) Protein sequence alignment of HPL-1 (Uniprot ID: G5EET5), HPL-2a (Uniprot ID: GSEDE2-1), HPL-2b (Uniprot ID: G5EDE2-2) and HPL-2c (Uniprot ID: G5EDE2-3). CD depicted by red chart. CSD indicated in green chart. Identical amino acids are highlighted in dark blue. Alignment performed by <https://www.uniprot.org>.

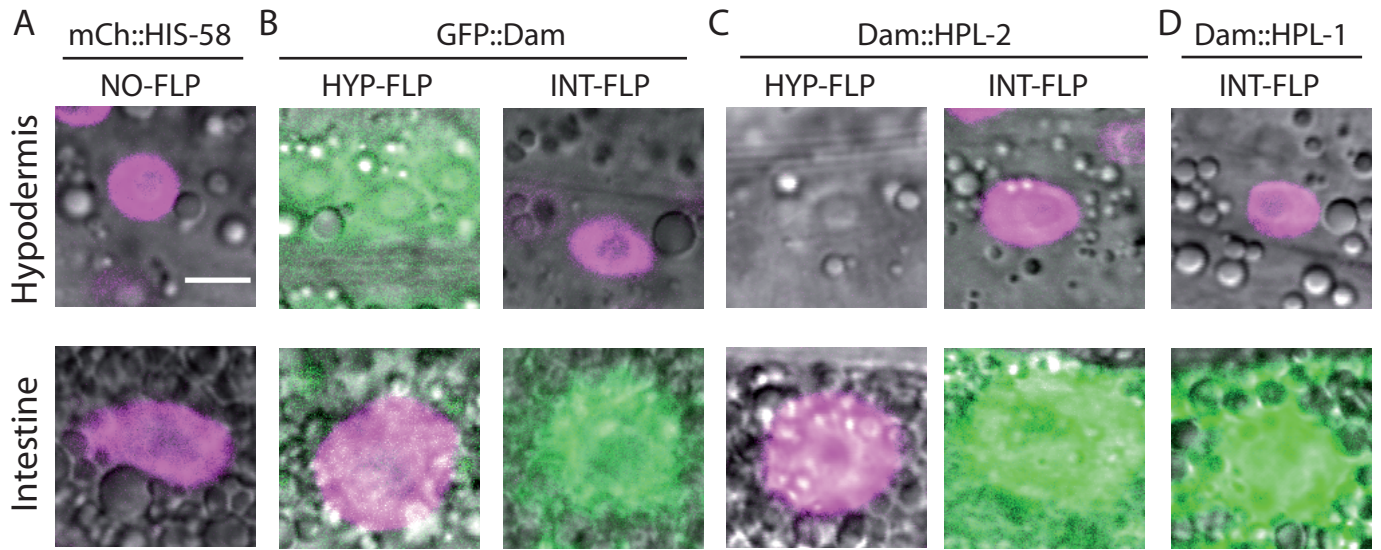
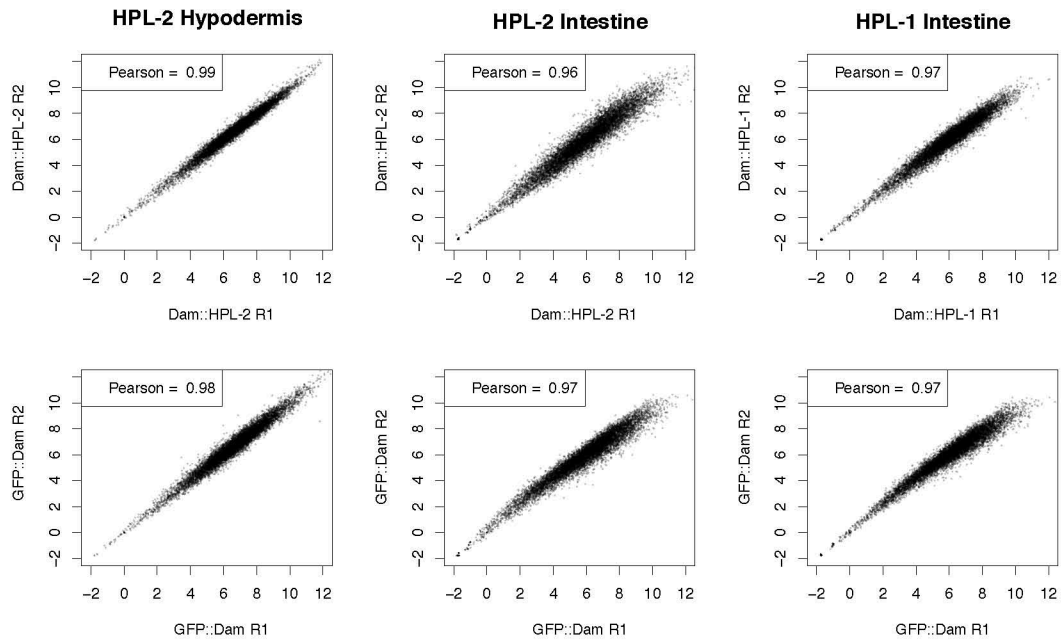


Figure S2. Tissue specificity of the DamID system in hypodermis and intestine. (A) In the absence of Flipase (NO-FLP), the mCherry::*his-58* (mCh::HIS-58) cassette is expressed in all tissues (shown in magenta). (B) GFP::Dam control strains. FLP expression in the hypodermis (HYP-FLP, left panels) or the intestine (INT-FLP, right panels) results in the excision of the mCherry::*his-58* cassette in that tissue and expression of the GFP::Dam fusion protein (shown in green). Expression of mCh::HIS-58 can be observed in the nuclei where FLP is absent. (C-D) Strains used for tissue-specific HPL-1/2 DamID. (C) Expression of FLP in hypodermis (HYP-FLP, left panels) or intestine (INT-FLP, right panels) results in the expression of Dam::HPL-2 in the tissue of interest after excision of the mCherry::*his-58* cassette. mCh::HIS-58 can be seen in the other tissue. (D) Dam::HPL-1 expression in the intestine is driven by intestinal FLP (INT-FLP) expression, resulting in the absence of mCh::HIS-58 specifically in that tissue. Note that in B-D INT-FLP is co-expressed with soluble mNeonGreen, which results in green intestinal nuclei and cytoplasm. Exhaustive evaluations of the two FLP drivers and their recombination efficiency and specificity on an identical FRT-flanked mCherry::*his-58* cassette also inserted into ttTi5605 on chrII were previously reported (MUÑOZ-JIMÉNEZ et al. 2017; FRAGOSO-LUNA et al. 2023). Bar: 5 μ m.

A



B

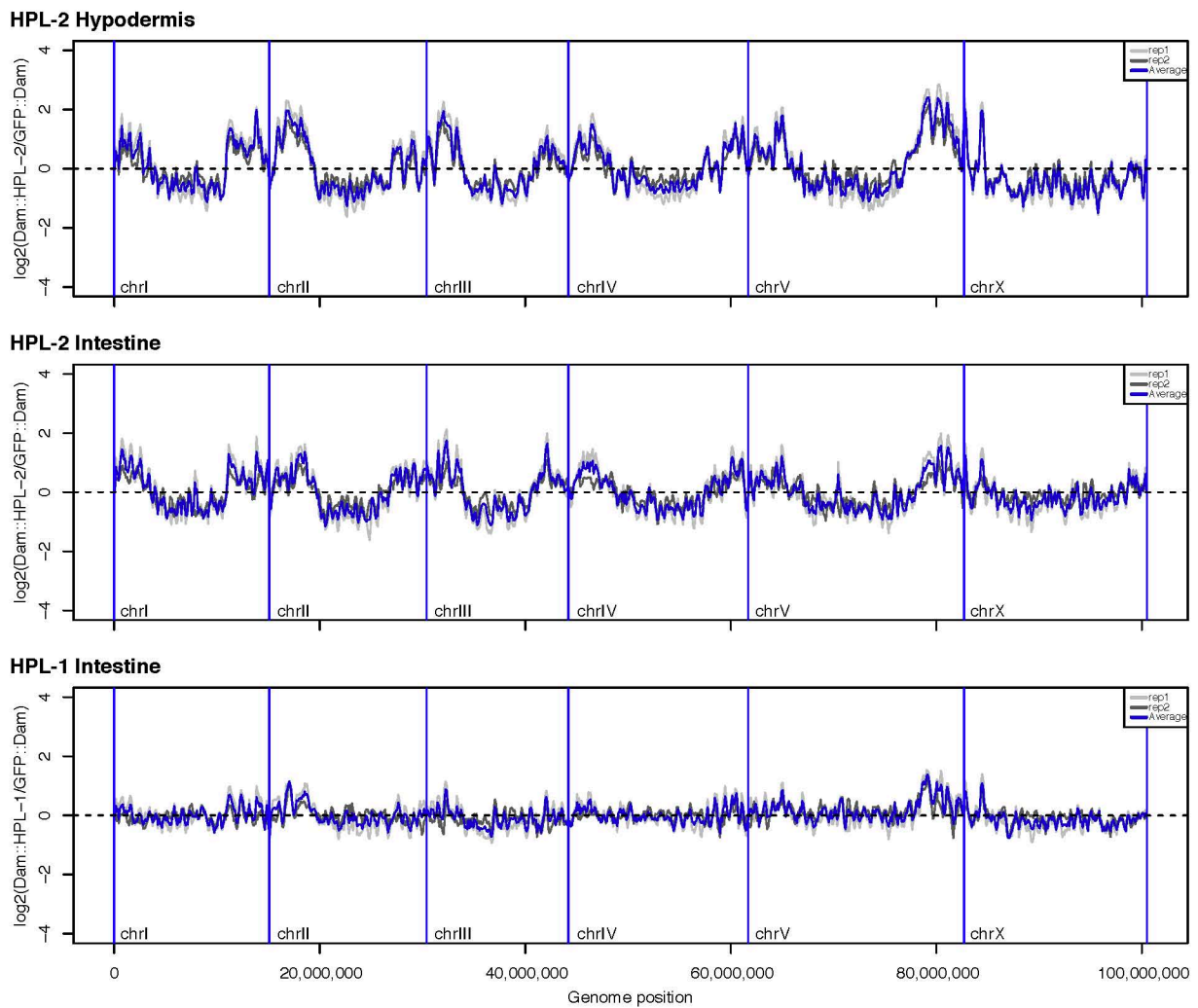


Figure S3. High correlation between DamID replicas. (A) Absolute read numbers per 10kb bin were transformed using the regularized log (rlog) function of the DESeq2 R package (version 1.36.0; (LOVE et al. 2014)). Pearson correlation values for each pair of transformed replicas are indicated in upper left corners. (B) Genome-wide $\log_2(\text{Dam::HPL}/\text{GFP::Dam})$ profiles at 100kb bin level. Individual replicas are represented in different tones of grey; average values are represented in blue. To facilitate visualization of the entire genome, the lines represent the rolling mean across 3 bins.

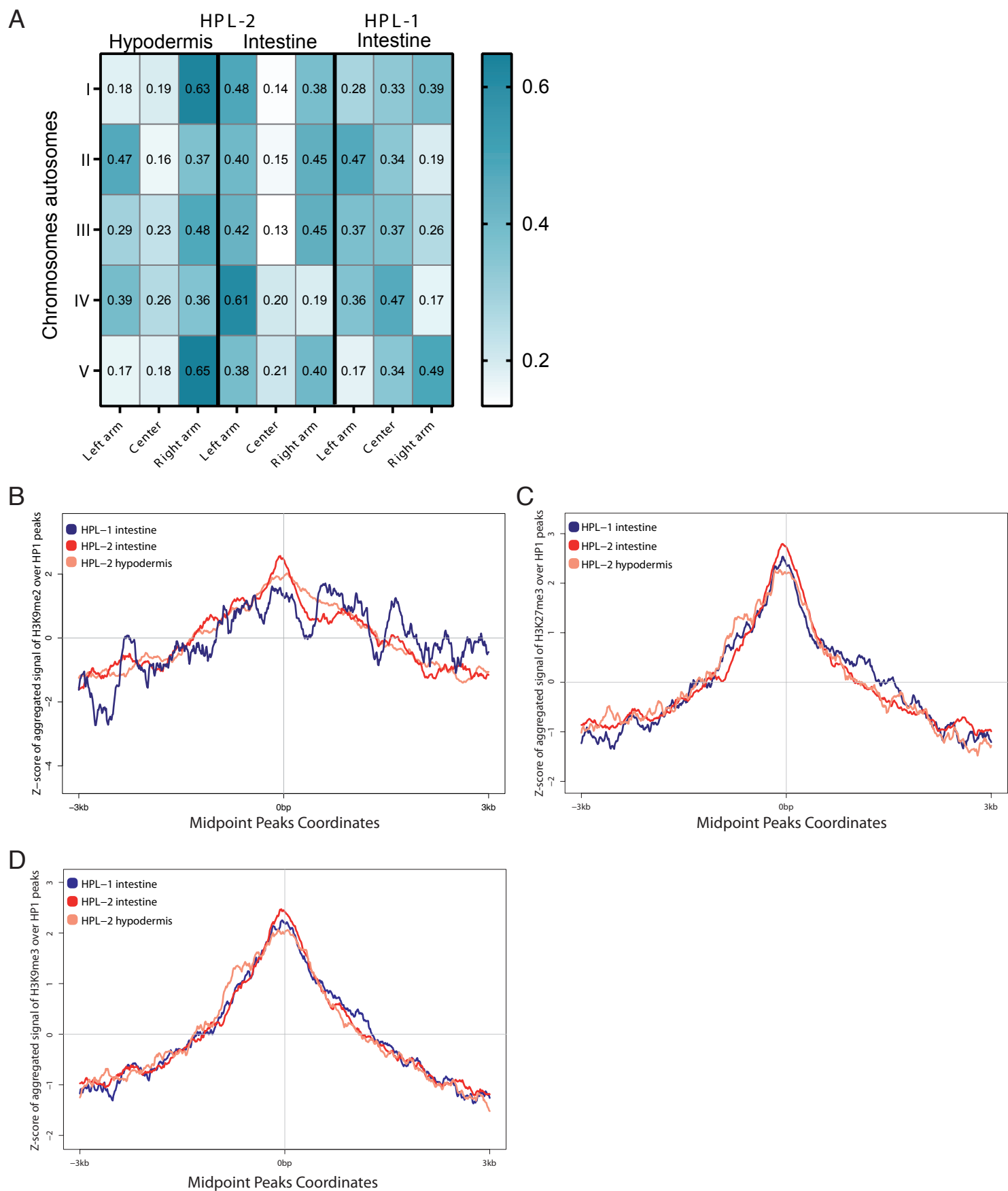


Figure S4. Tissue-specific chromatin binding of HPL-1 and HPL-2 and their association to histone marks.

(A) Heatmap depicting the proportion of HP1 peaks distributed by chromosomes autosomes distinguishing between arms and center. Chromosomes autosomes coordinates based on (GARRIGUES et al. 2015). (B-D) Aggregation plots depicting the average signal tracks for H3K9me2 (B), H3K27me3 (C) and H3K9me3 (D) histone datasets over HP1 peaks. Center position represents the midpoint location of peaks. Regions up to 3 kb upstream and 3 kb downstream of the midpoint in 10 bp bins are shown.

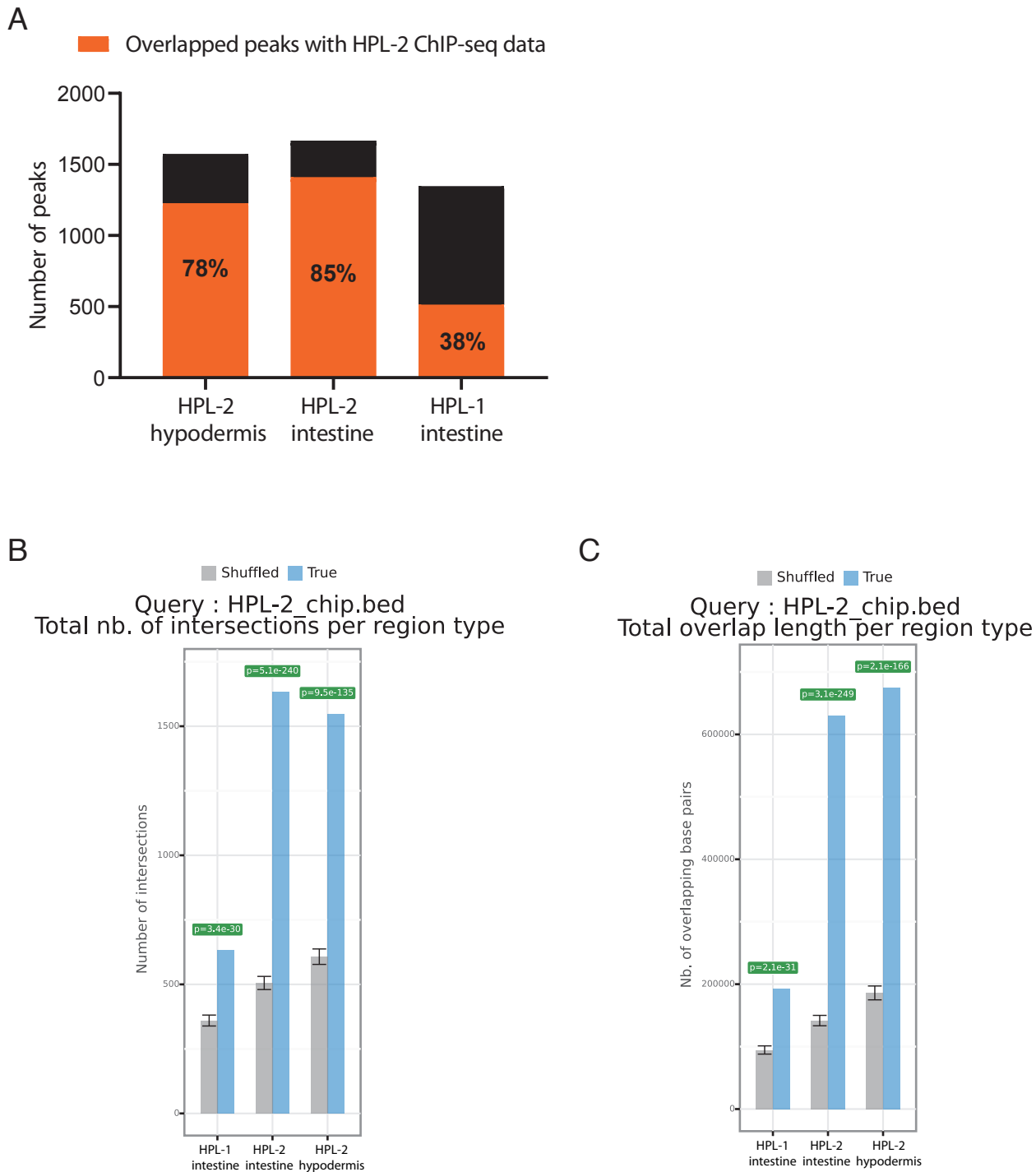


Figure S5. Overlapping of HP1 DamID and HPL-2 ChIP datasets. (A) Stacked plot depicting the number of overlapped peaks between HP1 datasets indicated and a published HPL-2 ChIP dataset. Numbers inside orange bars represent the proportion in percentage of overlapped peaks respect of total HP1 peaks number. (B-C) Statistics for overlapped peaks between HP1 and HPL-2 ChIP-seq using a Monte Carlo simulation, based on mathematical distributions of region (B) and inter-region lengths (C), according to negative binomial model of the total overlap length. Hpl-2_hyp: HPL-2 hypodermis; hpl-2_int: HPL-2 intestine; hpl-1_int: HPL-1 intestine.

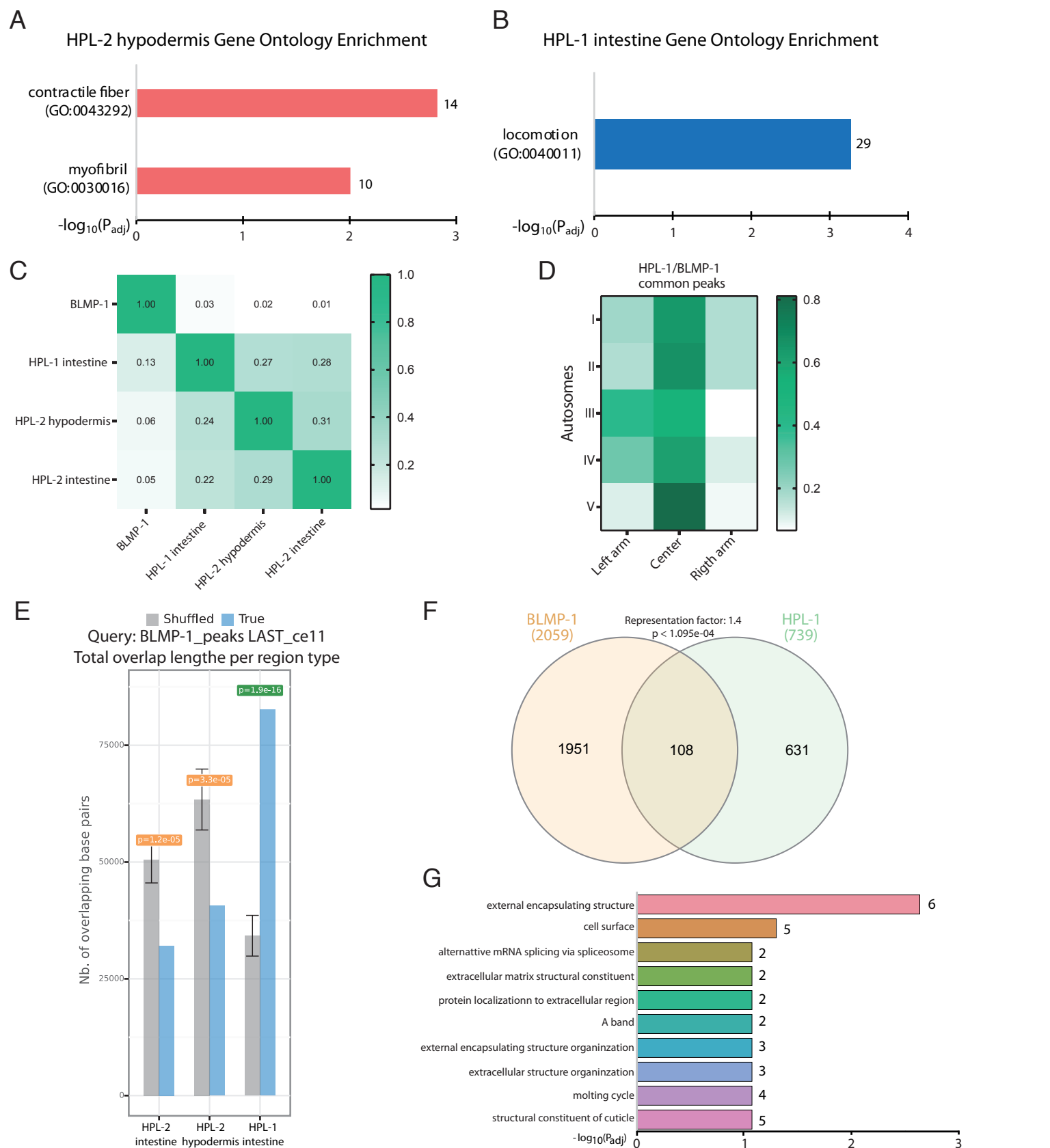


Figure S6. Differential tissue-specific binding of HP1 proteins. (A-B) GO terms associated to cellular component category of unique genes bound by HPL-2 in the hypodermal tissue (A) and by HPL-1 in the intestine (B). Number of intersected genes depicted in right side bars. (C) Heatmap depicting proportion of overlapped peaks between all datasets indicated. The number of BLMP-1 peaks is much higher than the number of HPL-1/2 peaks. Hence, the correlation values when querying with BLMP-1 peaks against HPL-1/2 peaks (top row) are lower than when querying with HPL-1/2 peaks against BLMP-1 peaks (left column). (D) Heatmap describing chromosome autosome location of overlapped peaks between BLMP-1 and HPL-1. (E) Number of intersected peaks between HP1 datasets and BLMP-1 assessed by Monte Carlo simulation statistical test. (F) Venn diagram indicating the number of overlapping genes between HPL-1 in the intestine and BLMP-1. Exact hypergeometric probability representation factor and p-value are shown. (G) Gene Ontology analysis of common genes bound by HPL-1 and BLMP-1. Number of intersected genes are depicted in right side bars. Only 35 out of 108 genes were considered.